Fatigue Failure Analysis Case Studies

Mehrooz Zamanzadeh and Edward Larkin
Exova, Pittsburgh, PA 15205
and
Reza Mirshams
Department of Engineering Technology
University of North Texas
Denton, TX 76207
Reza.Mirshams@unt.edu

ABSTRACT
Fatigue fracture can occur in many components such as: fasteners, and tubular pole structures. In this paper, fatigue failure mechanisms have been described and the application of the principles for failure analysis for each case will be presented. Cyclic loading at stresses above the fatigue limit of the material can initiate cracks at the surface or at internal defects. Macroscopic and microscopic observations of fatigue crack initiation and approaches for characterization of fatigue failures have been described. Two case studies present application of laboratory analysis techniques to determine primary causes and modes of failures.

Keyword: Fatigue; Fracture; steel; Weld; galvanized

1. Introduction

Metal characteristics can be changed due to the application of cyclic stress or strain and it can lead to the formation of cracks and eventual failure. The term fatigue has become a widely acceptable word in engineering material science for describing a particular mode of failure. Fatigue crack phenomena in metals is initiated by nucleation in at the nano- and micro- scales, leading to macroscopic crack growth and propagation, and ultimately to complete failure of a component or structure. Significant damage and the failure of machinery, welded structures, moving vehicles, and various mechanical systems can occur under fluctuating loads, and it requires a better understanding of the mechanisms of fatigue damage formation for planning strategies in engineering design, materials selection, and manufacturing processes to improve performance, extend fatigue life, and enhance safety of products. The combination of elevated temperatures or corrosive environments with variable loads intensifies fatigue damage. More complex fatigue damage formation has been observed in situations of mechanical contact between component surfaces in conjunction with repeated loads in rotating sliding systems. Selection of an appropriate mitigation process requires understanding fatigue damage mechanisms in materials and the fundamentals of engineering mechanics.

2. Evaluation of Fatigue Fracture

The early stages of failure analysis include the collection of background information and the selection of appropriate samples for laboratory testing. Additional steps should include site inspection, a timeline history of the failure, material specifications, review of maintenance and

repair records, number of past failures for the same component and any material substitutions made. A visual examination of the failed part or structure, as well as non-destructive testing of the component, with extensive photographic documentation should be performed first. The failed parts selected for laboratory testing and analysis should be carefully stored or protected during transport to prevent any damage to the fracture surfaces from humidity, dust, and dirt.

A macroscopic visual examination of the fracture surface and external surfaces of the part begins the investigation and will be followed by microscopic examinations. An optical stereo microscope examination at magnifications of 50X or less will help to reveal fracture surface details, confirm fracture initiation locations and mode of failure, and reveal possible evidence of surface damage at the locations of fatigue crack initiation. There are differences observed in fatigue fracture surface appearances caused by the magnitude of the applied stress and the remaining cross sectional area when the fracture passes through each area. The main differences are observed by macroscopic visual fractography. Fatigue fracture surfaces typically show two distinct regions: the fatigue crack initiation and propagation region and the final overload region. In the final overload region, the presence of slanted 45 degree shear zones and their elongated fibrous dimple structure, or brittle cleavage features are indicative of rapid loading conditions.

Metallographic examination by optical light microscopy in the range of 100x to 1000x is required to identify the microstructure and heat treat condition of the material, and to identify any possible defects originating from material processing or heat treatment. Many fatigue cracks can initiate from small defects. Scanning electron microscopy (SEM) would assist in characterization of type of fracture and pinpointing the source of crack initiation. Chemical analysis of the component will help to determine if the material has been heat treated for maximum strength as resistance to fatigue increases with increasing strength. The presence of alloying elements could be ascertained by scanning electron microscopy equipped with energy dispersive x-ray spectroscopy (EDS) for elemental analysis.

Mechanical properties should be verified and compared with specifications when available. Verification of mechanical properties assumes that the original design and material selection were correct but rules out incorrect material substitutions. Tensile tests should be performed if the size of the sample is sufficient. Hardness or microhardness testing can also be performed in lieu of tensile testing if the components are small, or if surface decarburization or carburization are present.

Analysis of the evidence collected is the final stage of a failure investigation. Identification of the fracture initiation site, defects or imperfections if present, size of the fatigue propagation zone compared with the size of the final failure zone, and material properties can be used to provide recommendations for corrective action. A final report including all relevant data, analysis, and recommendations is compiled and presented to the client. In litigation investigations, the client may not be interested in the recommendations section of the report.

3. Case Review: Broken Wheel Bolt

3.1. Introduction

A failure analysis investigation was performed on the broken steel bolts from an aluminum wheel hub from a truck trailer. The wheel hub contained eight metric steel bolts that had all failed in service causing the wheel to become separated from the trailer, Figure 1.

Figure 1: The aluminum wheel hub

3.2. Laboratory Examinations and Results

All examinations were made on the broken haves of the bolts after extracting them by cutting the hub. Also submitted were two non-broken bolts (NB) from a non-failed wheel of the same trailer as the broken bolts. The failure occurred on the front axle of a two axle heavy haul flatbed trailer. In addition, two new bolts from the same manufacturer (OEM) as the failed bolts and two new similar bolts from another manufacturer (AEM) were submitted for examination and comparison. All of the bolts were to conform to the requirements of ASTM F568M Grade 10.9 material. All of the bolts failed approximately 5/16 inch above the hub flange. The fracture surfaces and the fracture surface profiles for one of the broken bolts is shown in Figures 2.

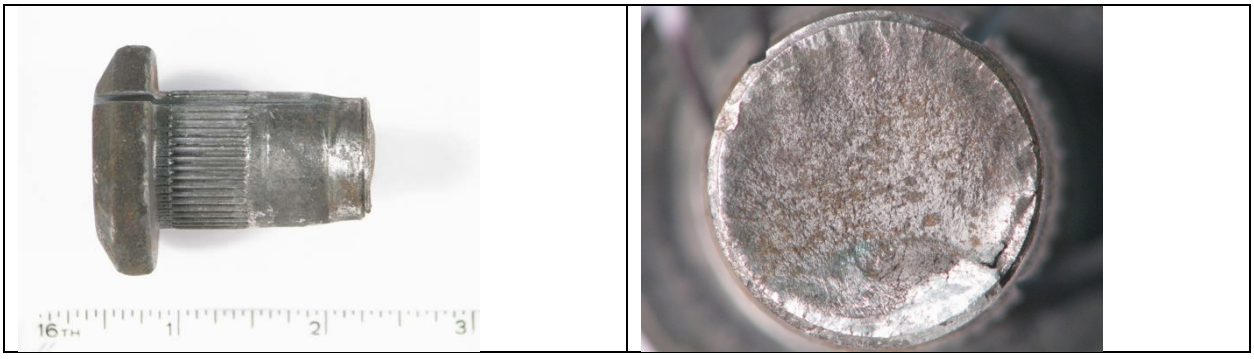

Figure 2: Photographs show one of the broken bolts and its fracture surface.

All of the bolt fractures were found to have initiated in the last thread root adjacent to the non-threaded shank. The primary fracture initiation location is at the top of the bolt fracture as shown in the photograph in Figure 2. The fracture surface profiles were observed to be relatively flat, or slightly concave, and perpendicular to the bolt axes. For five of the bolts, short radial ridges were observed to intersect the thread root at the fracture initiation locations.

These ridges represent steps between adjacent independent fracture initiation sites. These fracture surface features are characteristic of a fatigue mode of failure. The fracture surfaces of two bolts indicated that they had failed as a result of reverse bending fatigue with fractures initiating on opposite sides of the bolt diameters. Visual examination showed some fracture surfaces had initiated as a result of low cycle fatigue. It is apparent that the first bolts to fracture failed as a result of high cycle fatigue. Bolts which fractured second exhibited low cycle fatigue caused by greater stresses on the remaining bolts.

Bolts identified as non-failed, OEM and AEM were tested and all conformed to ASTM F568M Grade 10.9 requirements. Visual examinations of threads identified some corrosion in the non-broken bolts and wear along one of thread flanks. Nondestructive magnetic particle testing did not reveal any defects that would contribute to the initiation of the fatigue cracks. Screw pitches were measured using an optical comparator. All non-broken bolts were determined to have a thread pitch of 1.5 millimeters. The examination of thread roots and thread pitches did not indicate permanent stretching caused by over torqueing of the bolts.

Chemical analyses of all samples indicated that carbon contents of all bolts were approximately the same (0.42-0.44% wt.) which is slightly greater than the specified 0.40 maximum value of ASTM F568M grade 10.9.

Tensile testing of the non-broken bolts was performed in accordance with the methods of ASTM A370 and ASTM E8. The yield strength was determined at 2% offset and the results are given in the Table 1. All of the non-broken bolts conformed to the minimum tensile properties as specified in ASTM F568M for Grade 10.9 bolts. The broken bolts submitted were all too short to permit tensile testing.

Table 1: Tensile Test Properties

	New Bolt (AEM)	Bolt (NBB)	New Bolt (OEM)	ASTM F568M Grade 10.9
Yield Strength (psi)	149,000 (1027.3 MPa)	166,000 (1144.5 MPa)	162,000 (1116.9 MPa)	940 MPa Minimum (136,335 psi)
Tensile Strength (psi)	164,000 (1130.7 MPa)	172,000 (1185.9 MPa)	171,000 (1179.0 MPa)	1040 MPa Minimum (150,839 psi)
Percent Elongation in 0.2 Inches	14	16	17	---
Percent Reduction of Area %	46	57	65	---

Hardness testing was carried out on transverse cross sections for two broken bolts, three non-broken bolts identified as OEM, AEM and non-broken (NB) wheel from trailer. All surfaces were cut and ground to a 120 grit finish. Rockwell C scale hardness measurements were made on the cross sections at the center and mid-radius locations and the results are given in the Table 2.

All of the broken and non-broken bolts conformed to the hardness range specified in ASTM F568M for Grade 10.9 bolts.

Table 2: Rockwell C Scale Hardness Measurements

Sample (identification)	Measurements	Average	F568M Grade 10.9
New Bolt (AEM)	36.0 35.8 35.7 35.7 36.0	35.8	33-39
Non-broken Bolt (NB)	34.6 35.2 36.0 36.8 36.3	35.8	33-39
New Bolt (OEM)	35.3 35.8 36.0 36.0 37.1	36.0	33-39
Failed Bolts (Avg.)	32.0 35.9 36.0 37.6 36.6	35.6	33-39

Metallographic examinations were performed on transverse and longitudinal cross sections through the bolts. Standard metallographic sample preparation was used to prepare polished scratch free surfaces and etched with a 2% nital solution. Figure 3 shows the microstructure of a polished and etched section. A secondary crack in the bottom of a thread root and tempered martensitic microstructure are evident.

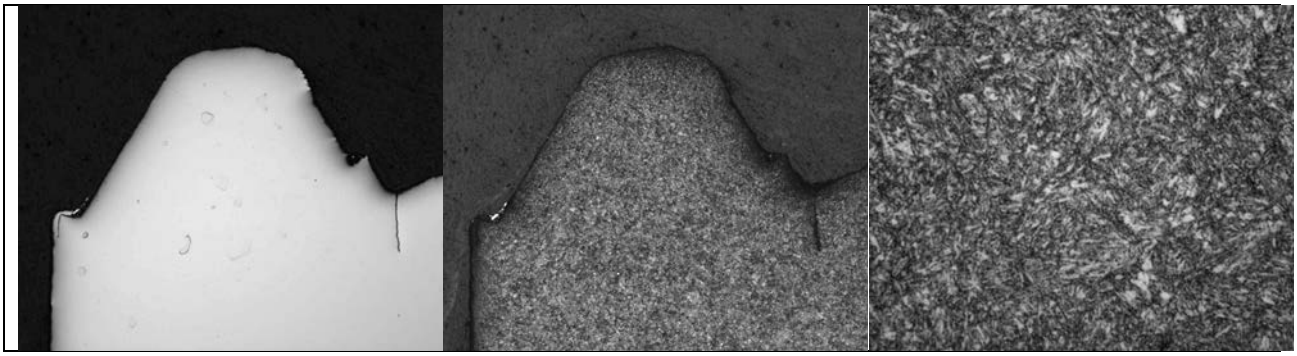

(a) 50x (b) 50x (c) 1000x

Figure 3: Photomicrographs of a broken bolt (a) a crack in bottom of thread root, (b) same section after etching with 2% nital, (c) the microstructure at higher magnification.

Transverse cross sections through the three non-broken bolts identified as New bolt (AEM), non-broken bolt (NB), and (OEM) bolt were also prepared for subsequent metallographic examination. The samples were examined in the as polished condition and etched with a 2% nital solution which revealed the microstructures.

Figure 4 presents micrographs of a non-broken bolt from the trailer with the broken wheel similar to the failed bolts. The threads were actually observed to have been bent to one side. Localized wear produced plastically deformed layers some of which appear white in these photographs. Such plastic deformation can produce hard, brittle surface layers. At one location a secondary internal crack was observed to have initiated at a large inclusion within a thread profile as shown in Figure 4 (b).

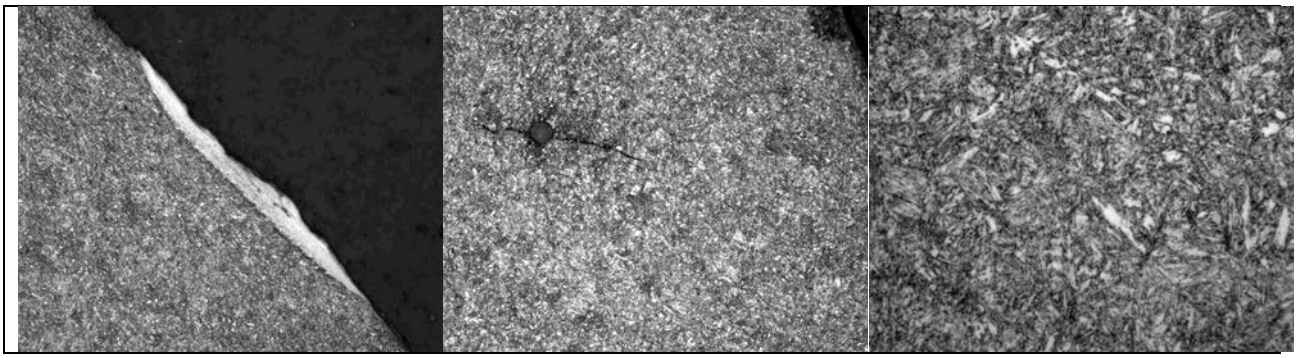

(a) 200x (b) 200x (c) 1000x

Figure 4: Photomicrographs of transverse cross section of the non-broken bolt (NBB) show (a) a localized wear area on the flank, (b) an internal crack initiating at an inclusion, and (c) tempered martensite microstructure.

3.3. Discussion and Conclusion

The broken bolts were found to have failed in service as a result of bending or reverse bending fatigue. All of the bolt fractures were found to have initiated in the last thread root adjacent to the non threaded shank. High cycle fatigue is the progressive failure of a component subjected to repeated or fluctuating strains at stresses less than the yield strength of the material. Low cyle fatigue generally occurs at stress levels which exceed the yield strength of the material. Fatigue cracks initiate at locations of maximum stress and/or minimum strength. Thread roots are a natural stress concentration site for the initiation of cracks.

All of the bolts tested, both broken and non-broken, did conform to the tensile and hardness properties specified in ASTM F568M for Grade 10.9 bolts. Although none of the bolts strictly conformed to the specified chemical requirements, the mechanical properties should be considered to be of more importance. Localized wear along the thread flanks was observed for the bolts that had been in service but had not failed. The gross plastic deformation of the threads observed during metallographic examination suggests that these bolts had been grossly over torqued during tightening. However, optical comparator measurements of the thread root to thread root distances in areas of thread deformation, and in areas of no thread deformation, revealed that no permanent stretching of the bolts had occurred.

There are generally two ways in which the tightening of bolts can contribute to fatigue failures. First, insufficient preloading can increase the stress excursions seen by the parts. This might occur if the bolts are not tightened enough. Preloading can also be lost if the bolts are tightened to such a degree that the bolts are stretched and plastically deformed by elongation. Second, excessive preloads caused by over tightening can increase residual stresses in the bolt, and the combination of residual stress plus applied stress in service can exceed the fatigue endurance limit of the material. We believe that this last scenario occurred for the broken bolts examined.

The New lot of bolts was observed to possess seams along the tooth flanks. Seams at the tops of the threads due to thread rolling are generally acceptable, if not too deep, because the

applied stresses in service are not active at these locations. However, seams (laps) originating on either flank and with a traverse (i.e. orientation) directed toward the interior and with a depth extending below the pitch line are non-permissible discontinuities as per Figure 6A of SAE J123. Seams along the thread flanks could lead to localized spalling if the bolts are tightened and untightened a number of times.

4. Case Review: Lightning Arrester Pole

4.1. Introduction

Galvanized poles are used for traffic signals, road signs, high-mast lighting and electrical transmission towers. Many failures of these types of structures can be attributed to fatigue and corrosion. According to National Cooperative Highway Research Program (NCHRP), most states have experienced, in one mode or other, failures of these support structures. Many others have experienced failures of high-mast luminary poles that are made of weathering steel or other materials. These failures are likely due to a lack of understanding of the behavior of materials and type of loadings. It is likely that these structures have been designed without considering the dynamic effects of wind, actual wind loads, modes of vibration, and others.

Lightning arresters are devices installed on electrical and telecommunication systems to protect them from damage due to lightning. The poles are made from galvanized coated steel and currently there is not an adopted standard for manufacturing, engineering design codes, or appropriate selection of materials. Recent incidents of failure of poles have made the Consumer Product Safety Commission (CPSC) call for the development of standards for design and manufacturing of lighting and electrical transmission towers and poles.

Typically, the arrestors are installed on electrical transmission towers or utility poles. Structural design of electrical power transmission poles should consider dynamic loadings due to wind and lightning in addition to static loads for the weight of cables and lightning arrester devices. The height of the poles can vary due to terrain and engineering constraints.

A utility lightning arrester pole with an approximate height of 110 feet had failed. The pole shaft was constructed from steel plate with a thickness of 0.212 inch in conformance with ASTM A572 Grade 55 steel. The base plate was specified to be in conformance with ASTM A36 steel with a maximum Carbon Equivalent of 0.45. Subsequent to manufacture the entire pole was hot dip galvanized. The pole failed during a high wind event and the following report is a determination of cause of failure.

4.2. Visual Examination

An examination of the fracture surface indicated that the fracture possessed two separate fatigue cracks in the pole shaft, as shown in Figure 5(a). The diameter of the lower part of shaft as shown in the figure 5(a) is 23 inches. The centers of the two crack lengths were diametrically opposite. This is characteristic of a reverse bending fatigue mode of failure. The failure occurred in the thinner pole shaft material immediately adjacent to the weld at the weld toe location.

The pole shaft possessed one longitudinal weld seam and one reinforced handhole and cover plate.

Figures 5(a) and 5(b) show areas of fatigue crack initiation where, because of geometry, the fatigue crack arrest marks are parallel to the outside diameter surface where the fracture initiated. Oxidation subsequent to the formation of the fatigue cracks has resulted in the visible dark bands in these photographs.

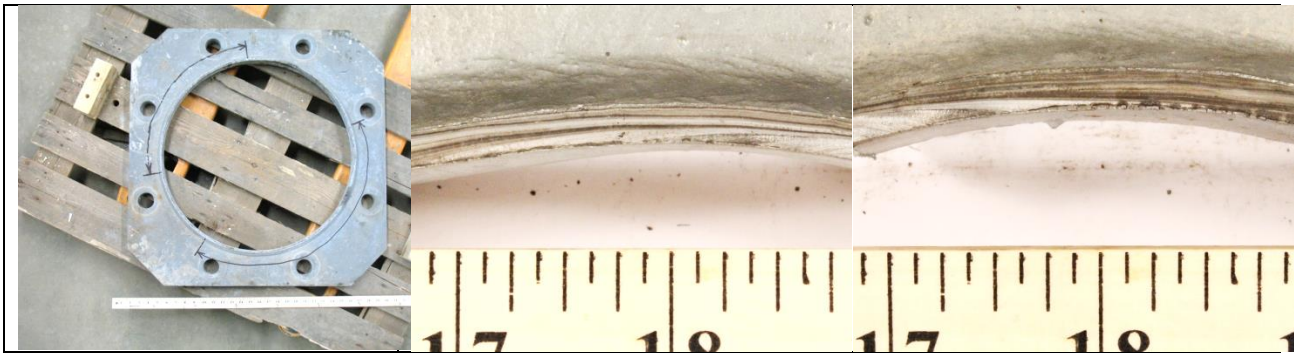

(a) (b) (c)

Figure 5: (a) Location and partial extent of the shorter (right) and longer (left) fatigue fractures in the pole shaft; (b) the fatigue crack arrest marks for the longer fatigue crack and (c) the fatigue crack arrest marks for the shorter fatigue crack.

4.3. Metallographic Examination

Transverse cross sections through the mating fracture surfaces of the longer fracture surface were prepared for subsequent metallographic examination. Etching with a 2% nital solution revealed the existing microstructures. The fracture occurred in the pole shaft at the weld toe location as shown in Figures 6(a) and 6(b).

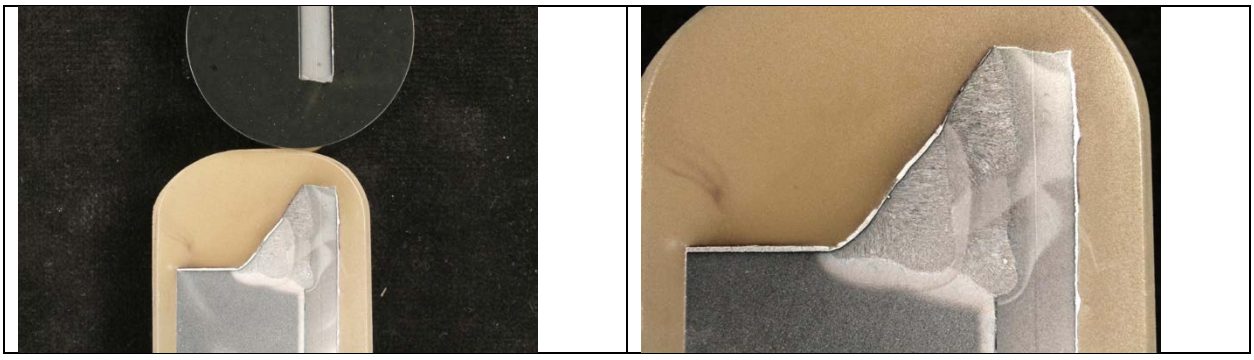

(a) (b)

Figure 6: Profile of through thickness of fracture on shaft and weld to the base plate.

The microstructure of the pole shaft heat affected zone (HAZ), at the weld toe location, consisted of fine grain ferrite plus dark etching bainite as shown in Figure 7a. The microstructure of the pole shaft away from the weld was found to consist of fine grained ferrite plus darker etching carbides. See Figures 7b and 7c.

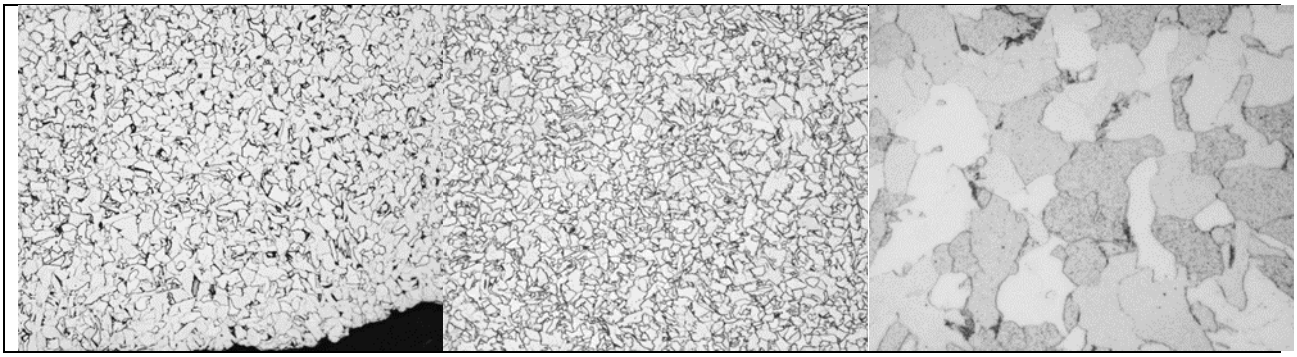

(a) 200x (b) 200x (c) 1000x

Figure 7: (a) the HAZ microstructure at the fracture surface. 2% nital; (b) the microstructure of the pole shaft. 2% nital; (c) the microstructure of the pole shaft. 2% nital.

4.4. Chemical Analysis

A quantitative chemical analysis was performed on the failed pole shaft and the results are given in the table below. The pole shaft conforms to the chemical requirements of ASTM A572 Grade 55 Type 2 Vanadium high strength low alloy (HSLA) steel and the supplemental requirement for low silicon content, as specified for hot dip galvanizing.

Table 3: Chemical Analysis

Element	Pole Shaft	A572 Type 2	Supplemental Spec
Carbon	0.065	0.25 Max	---
Manganese	0.85	1.35 Max	---
Phosphorus	0.013	0.04 Max	---
Sulfur	0.002	0.05 Max	---
Silicon	0.028	0.40 Max	0.06 Max
Chromium	0.056	---	---
Nickel	0.059	---	---
Molybdenum	0.005	---	---
Aluminum	0.031	---	---
Copper	0.11	---	---
Vanadium	0.053	0.01-0.15	---
Columbium	0.002	---	---
Titanium	<0.001	---	---
Nitrogen	0.016	---	---
Carbon Equivalent	0.245	---	---

4.5 Tensile Properties

A longitudinal tensile test specimen was machined from the pole shaft and tested in accordance with ASTM A370. The yield strength was determined at 0.2 percent offset and the results are given in the table below. The pole shaft conforms to the tensile property requirements of ASTM A572 Grade 55 steel, as specified.

Table 4: Tensile Properties

	Pole Shaft	**A572 Grade 55**
Yield Strength (psi)	71,800	55,000 Min
Tensile Strength (psi)	82,500	70,000 Min
Percent Elongation in 2 inches	26.1	20 Min

4.6. Conclusions

The lightning arrestor pole failed in service as a result of high cycle reverse bending fatigue that initiated in the pole shaft at the weld toe location. Two separate fatigue cracks were found to have initiated at diametrically opposites sides of the pole. This is characteristic of reverse bending fatigue. High cycle fatigue is the progressive failure of a component subjected to fluctuating strains at stresses less than the yield strength of the material. Fatigue cracks initiate at the locations of maximum local stress and/or minimum local strength. No weld defects, or other defects, were observed at the fracture initiation sites. The weld toe location is a natural geometric stress concentration site. The reported wind event at the time of failure served to topple a pole that already possessed two fatigue cracks. However, wind loading during the service life of the pole almost certainly is partly to blame for the fatigue failure. It is likely that these structures have been designed without considering dynamic effects of winds, actual wind loads, and modes of vibration.

Additional factors to consider are flatness and levelness of the pole base plate, the tightness of the nuts on the anchor bolts, and vibration of the pole during the lightning. The failed pole shaft was in conformance to the specified chemical and tensile property requirements of ASTM A572 Grade 55 material.

5. Bibliography

[1] S. Suresh, Fatigue of Materials, 2nd edition, Cambridge University Press, 1998.
[2] Jaap Schijve, Fatigue of Structures and Materials, Kluwer Academic Publishers, 2001.
[3] "Fatigue and Fracture," ASM Handbook Online, Volume 19, 1996.
[4] R.I. Stephens, A. Fatemi, R.R. Stephens, H.O. Fuchs, Metal Fatigue in Engineering, 2nd Ed., John Wiley & Sons, 2001.
[5] Y. Murakami and K.J. Miller, What is fatigue damage? A view point from the observation of low cycle fatigue process, International Journal of Fatigue, Volume 27, Issue 8, 2005, 991–1005.
[6] "Fractography," ASM Handbook, Vol. 12, 9th Ed., 1987.
[7] Derek Hall, Fractography, Cambridge University Press, 1999.
[8] Zamanzadeh, M., Kempkes, C., Aichinger, D., and Riley, D., "Laboratory and Field Corrosion Investigation of Galvanized Utility Poles," Electrical Transmission Line and substation Structures: 2006, pp. 235-249.
[9] Zamanzadeh, M., Gilpin-Jackson, A., "Corrosion Risk Strategies for Below-Grade Foundations of Transmission and Distribution Structures," Materials Performance, 2014, Vol. 35, 54-57.
[10] Thompson, Reilly William, "Evaluation of High-Level Lighting Poles Subjected to Fatigue Loading," 2012, *Theses and Dissertations.*

[11] Mina Dawood, Raka Goyal, Hemant Dhonde; and Timothy Bradberry, “Fatigue Life Assessment of Cracked High Mast Illumination Poles,” J. Perform. Constr. 2014, .28:311-320.